Cancer Research

PPARδ Elicits Ligand-Independent Repression of Trefoil Factor Family to Limit Prostate Cancer Growth

Natalia Martín-Martín[1,2], Amaia Zabala-Letona[1,2], Sonia Fernández-Ruiz[1,2], Leire Arreal[1], Laura Camacho[1,3], Mireia Castillo-Martin[4], Ana R. Cortazar[1,2], Verónica Torrano[1,2], Ianire Astobiza[1], Patricia Zúñiga-García[1], Aitziber Ugalde-Olano[2,5], Ana Loizaga-Iriarte[2,6], Miguel Unda[2,6], Lorea Valcárcel-Jiménez[1], Amaia Arruabarrena-Aristorena[1], Marco Piva[1], Pilar Sánchez-Mosquera[1], Ana M. Aransay[1,7], Antonio Gomez-Muñoz[3], Rosa Barrio[1], James D. Sutherland[1], and Arkaitz Carracedo[1,2,3,8]

Abstract

The nuclear receptor PPAR-β/δ (PPARD) has essential roles in fatty acid catabolism and energy homeostasis as well as cell differentiation, inflammation, and metabolism. However, its contributions to tumorigenesis are uncertain and have been disputed. Here, we provide evidence of tumor suppressive activity of PPARD in prostate cancer through a noncanonical and ligand-independent pathway. PPARD was downregulated in prostate cancer specimens. In murine prostate epithelium, PPARD gene deletion resulted in increased cellularity. Genetic modulation of PPARD in human prostate cancer cell lines validated the tumor suppressive activity of this gene *in vitro* and *in vivo*. Mechanistically, PPARD exerted its activity in a DNA binding-dependent and ligand-independent manner. We identified a novel set of genes repressed by PPARD that failed to respond to ligand-mediated activation. Among these genes, we observed robust regulation of the secretory trefoil factor family (TFF) members, including a causal and correlative association of TFF1 with prostate cancer biology *in vitro* and in patient specimens. Overall, our results illuminate the oncosuppressive function of PPARD and understanding of the pathogenic molecular pathways elicited by this nuclear receptor.

Significance: These findings challenge the presumption that the function of the nuclear receptor PPARβ/δ in cancer is dictated by ligand-mediated activation. *Cancer Res; 78(2); 399–409. ©2017 AACR.*

Introduction

In the process of cellular transformation, cancer cells exhibit profound changes in nutrient uptake and utilization as a way to generate substrates for the production of biomass. This metabolic switch in cancer cells involves rewiring of cellular signaling and reprogramming of metabolic pathways. One of the main triggers for metabolic reprogramming is the alteration in cancer genes that remodel the signaling landscape (1). Seminal investigations have demonstrated that most cancer cells reprogram their metabolism to increase glucose uptake for glycolysis and decrease the flux toward TCA cycle and oxidative phosphorylation, using additional nutrients for anabolism. We have recently demonstrated that the regulation of metabolism downstream nuclear receptors affects prostate cancer progression and metastasis (2). More importantly, this study demonstrates for the first time that genetic events such as PGC1α alteration can trigger metabolic reprogramming in prostate cancer. Prostate cancer is the fifth leading cause of death by cancer worldwide (3), second in the male population, and it has been related to changes in glucose metabolism and lipid biosynthesis. However, the contribution of fatty acid oxidation (FAO) pathways to the pathogenesis and progression of prostate cancer remained obscure.

The family of peroxisome proliferator-activated receptors (PPAR) plays a central role in metabolic regulation, but their role in cancer is yet to be clarified (4, 5). In particular, PPAR β/δ (PPARδ, *PPARD*) is a transcription factor that belongs to this family of nuclear receptors that control target gene expression in response to endogenous and exogenous ligands (6, 7). PPARδ is constitutively expressed in tissues (7), and its canonical transcriptional activity relies on heterodimeric binding to PPAR response elements (PPRE) with a retinoid X receptor (RXR) moiety (8, 9). This activity is relevant for cell differentiation, macrophage activation, and cancer (10). The contribution of PPARδ in tumor biology through the regulation of multiple pathways (i.e., proliferation, apoptosis, wound healing, invasion, or migration) remains controversial and has been summarized in recent reviews (10, 11). Three primarily modes

[1]CIC bioGUNE, Bizkaia Technology Park, Derio, Spain. [2]CIBERONC, Madrid, Spain. [3]Biochemistry and Molecular Biology Department, University of the Basque Country (UPV/EHU), Bilbao, Spain. [4]Champalimaud Centre for the Unknown, Portugal. [5]Department of Pathology, Basurto University Hospital, Bilbao, Spain. [6]Department of Urology, Basurto University Hospital, Bilbao, Spain. [7]Centro de Investigación Biomédica en Red de Enfermedades Hepáticas y Digestivas (CIBEREHD), Madrid, Spain. [8]IKERBASQUE, Basque Foundation for Science, Bilbao, Spain.

Note: Supplementary data for this article are available at Cancer Research Online (http://cancerres.aacrjournals.org/).

Corresponding Author: Arkaitz Carracedo, CIC bioGUNE, Bizkaia Technology Park 801A bld., 48160, Derio, Spain. Phone: 34-94-406-13-08; Fax: 34-94-406-13-01; E-mail: acarracedo@cicbiogune.es

doi: 10.1158/0008-5472.CAN-17-0908

of regulation by PPARδ have been described (12, 13): (i) canonical ligand-induced activation and/or derepression by PPARδ, (ii) ligand-independent repression by PPARδ, and (iii) ligand-independent activation by PPARδ.

In the current study, we ascertained the biological activity of PPARδ in prostate cancer. Our results reveal that PPARδ exerts a tumor suppressive activity that is independent of ligand-mediated activation. Furthermore, we show that repression of trefoil factor family (TFF) member 1 (TFF1) is causal to the biological function of PPARδ. This study opens a new avenue in the biological activity of PPARδ that might lead to the identification of novel pathophysiologic functions of this nuclear receptor.

Materials and Methods

Reagents

Doxycycline (Sigma) was used at different doses to induce the expression of cDNA or shRNA from TRIPZ. GW501516 (Enzo Life Sciences; ALX-420-032-M001) was dissolved in DMSO and used at 0.1 μmol/L concentration. GW0742 and L165,041 (Tocris, refs. 2229 and 1856, respectively) were dissolved in DMSO and used at 1 μmol/L concentration. Etomoxir (Sigma) dissolved in water and used at 200 μmol/L concentration. Recombinant human TFF1 protein (R and D systems) was dissolved in PBS at 100 μmol/L and used at 1 μmol/L final concentration.

Patient samples

All samples were obtained from the Basque Biobank for research (BIOEF, Basurto University Hospital) upon informed consent and with evaluation and approval from the corresponding ethics committee (CEIC-E code OHEUN11-12 and OHEUN14-14). The patient studies were conducted in accordance with the ethical guidelines from the Declaration of Helsinki.

Cell culture

DU145, PC3, LNCAP, PWR1E, VCAP, C4-2, and 22RV1 cell lines were obtained from the ATCC or from Leibniz-Institut—Deutsche Sammlung von Mikroorganismen und Zellkulturen GmbH (DMSZ), who provided an authentication certificate, and the identity was validated by microsatellite analysis. None of the cell lines used in this study was found in the database of commonly misidentified cell lines maintained by ICLAC and NCBI Biosample. All cell lines were routinely monitored for *mycoplasma* contamination and quarantined while treated if positive. DU145, PC3, and VCAP cell lines were maintained in DMEM media supplemented with 10% (v/v) fetal bovine serum (FBS) and 1% (v/v) penicillin–streptomycin. The 22RV1, LNCAP, and C4-2 cell lines were maintained in RPMI media supplemented with 10% (v/v) FBS and 1% (v/v) penicillin–streptomycin.

Generation of stable cell lines

293FT cells were used for lentiviral production. Lentiviral vectors expressing shRNAs against human *PPARD* and human *TFF1* from the Mission shRNA Library were purchased from SigmaAldrich. Cells were transfected with lentiviral vectors following standard procedures, and viral supernatant was used to infect cells. Selection was done using puromycin (2 μg/mL) for 48 hours. As a control, a lentivirus expressing scrambled shRNA (shC) was used. Short hairpins sequence: shC: CCGGCAACAAGATGAAGAGCACCAACTCGAGTTGGTGCTCTTCATCTTGTTG; sh#64 against PPARD: CCGGCCGCAAACCCTTCAGTGATATCTCGAGATATCACTGAAGGGTTTGCGGTTTTT and sh#50 against TFF1: CCGGTATCCTAATACCATCGACGTCCTCGAGGACGTCGATGGTATTAGGATATTTTTG. pBabe-puro was a gift from Hartmut Land & Jay Morgenstern & Bob Weinberg; Addgene plasmid #1764 (14), pBabe puro PPAR delta was a gift from Bruce Spiegelman; Addgene plasmid #8891 (15). Point mutations of *PPARD* DNA binding motif (two conserved cysteine residues, Cys-90 and Cys-93, were mutated to alanines) were created by site-directed mutagenesis by using a Quick change site-directed mutagenesis kit (Stratagene) as reported (16). HA-PPARD inducible system was constructed by cloning *PPARD* into TRIPZ vector as reported (2). Briefly, HA-PPARD was subcloned using Age1 and Mlu1 sites into a TOPO cloning vector and then transferred to TRIPZ vector. PPARD targeting shRNA was subcloned from pSM2c (Open Biosystems, #5467) using XhoI and MluI sites into a TRIPZ vector. *TFF1* was amplified from human cDNA pool (heart/thyroid mix) using primers TZ.Age.TFF1.for and TZ.Mlu.pA.TFF1.rev, and inserted into TRIPZ (Age1-Mlu1) using Gibson cloning. Final clone was confirmed by Sanger sequencing. Sequences are available by request.

Western blotting

Western blot analysis was carried out as previously described (17). Briefly, cells were seeded on 6-well plates and 4 days (unless otherwise specified) after seeding cell lysates were prepared with RIPA buffer (50 mmol/L TrisHCl pH 7.5, 150 mmol/L NaCl, 1 mmol/L EDTA, 0.1% SDS, 1% Nonidet P40, 1% sodium deoxycholate, 1 mmol/L sodium fluoride, 1 mmol/L sodium orthovanadate, and 1 mmol/L beta-glycerophosphate and protease inhibitor cocktail; Roche). The following antibodies were used for Western blotting: mouse monoclonal anti-PPARδ, 1:500 dilution (Santa Cruz Biotechnology, F7, sc-74440) for detection of endogenous PPARδ, rabbit polyclonal anti-PPARδ, 1:1,000 dilution (Santa Cruz Biotechnology, K20: sc-1987) for exogenous protein, rabbit polyclonal anti-caveolin-1, 1:2,000 (BD Biosciences, Cat. No. 610059), rabbit monoclonal anti-TFF1, 1:1,000 (Cell Signaling Technology, 15571), rabbit polyclonal anti-HSP-90, 1:1,000 (Santa Cruz Biotechnology, sc-4874), rabbit polyclonal anti-GAPDH, 1:1,000 (Santa Cruz Biotechnology, sc-2118) and mouse monoclonal anti-beta-Actin 1:2,000 dilution (clone: AC-74, catalog: A5316, Sigma-Aldrich). After standard SDS-PAGE and Western blotting techniques, proteins were visualized using the ECL system.

Histopathologic analysis

After euthanasia, histologic evaluation of a hematoxylin and eosin (H&E)–stained section from formalin-fixed paraffin-embedded prostate tissues was performed. After histopathologic evaluation, quantitative assessment of the prostate glandular structures by counting the number of epithelial cells in 5 high power fields (total area of 0.431 mm^2) of representative zones of the prostate was performed. Mean number of cells per mm^2 was compared between wild-type and $PPARD^{pc-/-}$ mice at different ages (9 $PPARD^{pc-/-}$ mice with ages: 9–12 months; 10 $PPARD^{pc-/-}$ mice with ages: 18–20 months; 16 wild-type mice with ages: 9–12 months; 11 wild-type mice with ages: 18–20 months).

Quantitative real-time PCR

Cells were seeded as for Western blot. Total RNA was extracted from cells using a NucleoSpin RNA isolation kit from Macherey-

Nagel (ref: 740955.240C). cDNA was produced from 1 μg of RNA using qScript cDNA SuperMix (Quanta Bioscience, ref: 95048). Taqman probes were obtained from Applied Biosystems. Amplifications were run in a Viia7 or QS6 Real-Time PCR System (Applied Biosystems) using the following probes: *PPARD* (Hs04187066_g1, cat: 4331182). For *ADFP*, *PDK4*, *ANGPTL4*, *Caveolin-1*, *TFF1*, *TFF2 and TFF3* amplification, Universal Probe Library (Roche) primers and probes were used (*ADFP*, For: tcagctccattctactgttcacc, Rev: cctgaattttctgattggcact; probe: 72; *PDK4*, For: cagtgcaattggttaaaagctg, Rev: ggtcatctgggcttttctca; probe: 31; *ANGPTL4*, For: gttgacccggctcacaat, Rev: ggaacagctcctggcaatc; probe: 44; *CAV-1* For: aacacgtagctgcccttcag, Rev: ggatgggaacggtgtagagat, probe: 24; *TFF1*, For: gatccctgcagaagtgtctaaaa, Rev: cccctggtgcttctatccta, probe: 35; *TFF2*, For: ccagatgcatcctctggaac, Rev: ggaagtgctgcttctccaac, probe: 37; *TFF3*, For: tggaggtgcctcagaaggt, Rev: gctgctgctttgactccag, probe: 4). *β-Actin* (Hs99999903_m1, cat: 4331182) and *GAPDH* (Hs02758991_g1, cat: 4331182) housekeeping assays from Applied Biosystems showed similar results (all qRT-PCR data presented were normalized using *GAPDH*).

Cellular assays

FAO and soft-agar colony formation were performed as previously described (2). Relative invasive growth experiments were carried out plating 700 cells upside down in suspension in 20% methylcellulose medium drops. A sphere was formed in every individual drop, and thus was considered a biological replicate. After 3 days, when the spheres were formed, they were embedded in a collagen based medium (55% collagen I, 20% DMEM 5×, 21.3% H_2O and 3% 0.1 N NaOH), and photos were taken after collagen polymerization (0-hour time point). After 16 hours, photos were taken again and the relative invasive growth was calculated with the relative area increase.

Mice

Xenograft experiments were carried out following the ethical guidelines established by the Biosafety and Welfare Committee at CIC bioGUNE and in accordance with an Institutional Animal Care and Use Committee. The procedures used were carried out following the recommendations from AAALAC. Xenograft experiments were performed as previously described (2), injecting either 3×10^6 (*PPARD* silencing and *TFF1* ectopic expression) or 3×10^5 (*PPARD* ectopic expression) cells per condition (unless otherwise specified), two to four injections per mouse. All mice (male Hsd:Athymic Nude-Foxn1 nu/nu) were inoculated at 8 to 12 weeks of age. The $Ppard^{Floxed}$ conditional knockout allele has been described elsewhere (18). Prostate epithelium-specific deletion was effected by the Pb-Cre4 (19). Mice were fasted for 6 hours prior to tissue harvest (9 am–3 pm) in order to prevent metabolic alterations due to immediate food intake.

Chromatin immunoprecipitation

Chromatin immunoprecipitation (ChIP) was performed using the SimpleChIP Enzymatic Chromatin IP Kit (Cat: 9003, Cell Signaling Technology, Inc.). PC3 cells were grown in 150-mm dishes either with or without 500 ng/mL doxycycline during 3 days. Cells from three 150 mm dishes (2.5×10^7 cells) were cross-linked with 35% formaldehyde for 10 minutes at room temperature. Glycine was added to dishes, and cells incubated for 5 minutes at room temperature. Cells were then washed twice with ice-cold PBS and scraped into PBS + PMSF. Pelleted cells were lysed and nuclei were harvested following the manufacturer's instructions. Nuclear lysates were digested with micrococcal nuclease for 20 minutes at 37°C and then sonicated in 500 μL aliquots on ice for 3 pulses of 15 seconds using a Branson sonicator. Cells were held on ice for at least 1 minute between sonications. Lysates were clarified at 11,000 × *g* for 10 minutes at 4°C, and chromatin was stored at −80°C. HA-Tag polyclonal antibody (Cat: C29F4, Cell Signaling Technology) and IgG antibody (Cat: 2729, Cell Signaling Technology) were incubated overnight (4°C) with rotation and protein G magnetic beads were incubated 2 hours (4°C). Washes and elution of chromatin were performed following the manufacturer's instructions. DNA quantification was carried out using a Viia7 Real-Time PCR System (Applied Biosystems) with SybrGreen reagents and primers that amplify the predicted PPARδ binding region to *TFF1* or *TFF3* promoter or to region of the promoter of PPARD canonical target genes containing the canonical PPARD DNA binding domain (as shown in Supplementary Table S1).

Transcriptomic analysis

For transcriptomic analysis in empty-vector–transduced PC3 cells and *PPARD*-expressing counterparts, the Illumina whole-genome -HumanHT-12_V4.0 (DirHyb, nt) method was used as reported previously (2). Probes not detected in at least one sample ($P > 0.01$) were excluded for subsequent analyses as they are considered to represent transcripts that are not expressed. For the detection of differentially expressed genes, a linear model was fitted to the data, and empirical Bayes moderated t-statistics were calculated using the limma package from Bioconductor. Adjustment of *P* values was done by the determination of false discovery rates (FDR) using Benjami–Hochberg procedure. Establishment of differentially expressed genes was based on fold change (fc) ≥ 1.5 or ≤ -1.5 and adjusted *P* value ≤ 0.05.

Data availability

Transcriptomics data are available at GEO (GSE95054). The link for the reviewers is provided At https://www.ncbi.nlm.nih.gov/geo/query/acc.cgi?token=glcvicamrtelngd&acc=GSE95054.

Statistics and reproducibility

No statistical method was used to predetermine sample size. The experiments were not randomized. The investigators were not blinded to allocation during experiments and outcome assessment. Unless otherwise stated, data analyzed by parametric tests are represented by the mean ± SEM of pooled experiments and median ± interquartile range for experiments analyzed by nonparametric tests. N values represent the number of independent experiments performed, the number of individual mice or patient specimens. For each independent *in vitro* experiment, at least three technical replicates were used and a minimum number of three experiments were performed to ensure adequate statistical power. In the *in vitro* experiments, normal distribution was assumed and one sample *t* test was applied for one-component comparisons with control and Student *t* test for two-component comparisons. For *in vivo* experiments as well as for experimental analysis of human biopsies (from Basurto University Hospital), a nonparametric Mann–Whitney exact test was used. Spearman rank correlation coefficient was applied for correlation analysis for samples not following a normal distribution. The confidence level

used for all the statistical analyses was of 95% (alpha value = 0.05). Two-tailed statistical analysis was applied for experimental design without predicted result, and one-tail for validation or hypothesis-driven experiments.

Results

PPARδ inhibits prostate cancer aggressiveness

In order to elucidate the contribution of PPARδ to prostate cancer biology, we first undertook an *in vivo* approach. We evaluated *PPARD* mRNA (11 benign prostate hyperplasia and 16 primary prostate cancer tissue extracts harvested following the guidelines reported; ref. 20) in human specimens. The results revealed a significant downregulation of *PPARD* in cancerous tissues compared with benign disease (Fig. 1A). Importantly, these results were corroborated in publicly available datasets using Oncomine (21; Supplementary Table S2). Next, we deleted *Ppard* conditionally in the mouse prostate epithelium using Probasin-Cre4 promoter (19), which led to increased cellularity both in adult (9–12 months old) and aged (18–20 months old) mice (Fig. 1B–D).

These results are supportive of an oncosuppresive role of PPARδ in prostate cancer and prompted us to characterize the biological and molecular consequences of *PPARD* manipulation in experimental systems. Using benign immortalized prostate cells (PWR1E) as a baseline, we identified prostate cell lines with elevated (DU145) or reduced (PC3, LNCAP) expression of PPARδ, so we chose these to genetically manipulate PPARδ levels (Supplementary Fig. S1A–S1C). DU145 cells were subject to *PPARD* silencing by means of constitutive (pLKO, sh64; Supplementary Fig. S1D–S1F) or inducible (TRIPZ-shPPARD) expression of short hairpin (sh) RNAs against *PPARD* gene (different hairpin sequences were used to exclude off-target effects; Supplementary Fig. S1G). In coherence with the *in vivo* data, *PPARD* silencing resulted in increased aggressiveness features of DU145 cells, namely soft-agar colony formation and invasive growth (Fig. 1E and F; Supplementary Fig. S1H). Importantly, *PPARD* silencing-induced prostate cancer aggressiveness was confirmed *in*

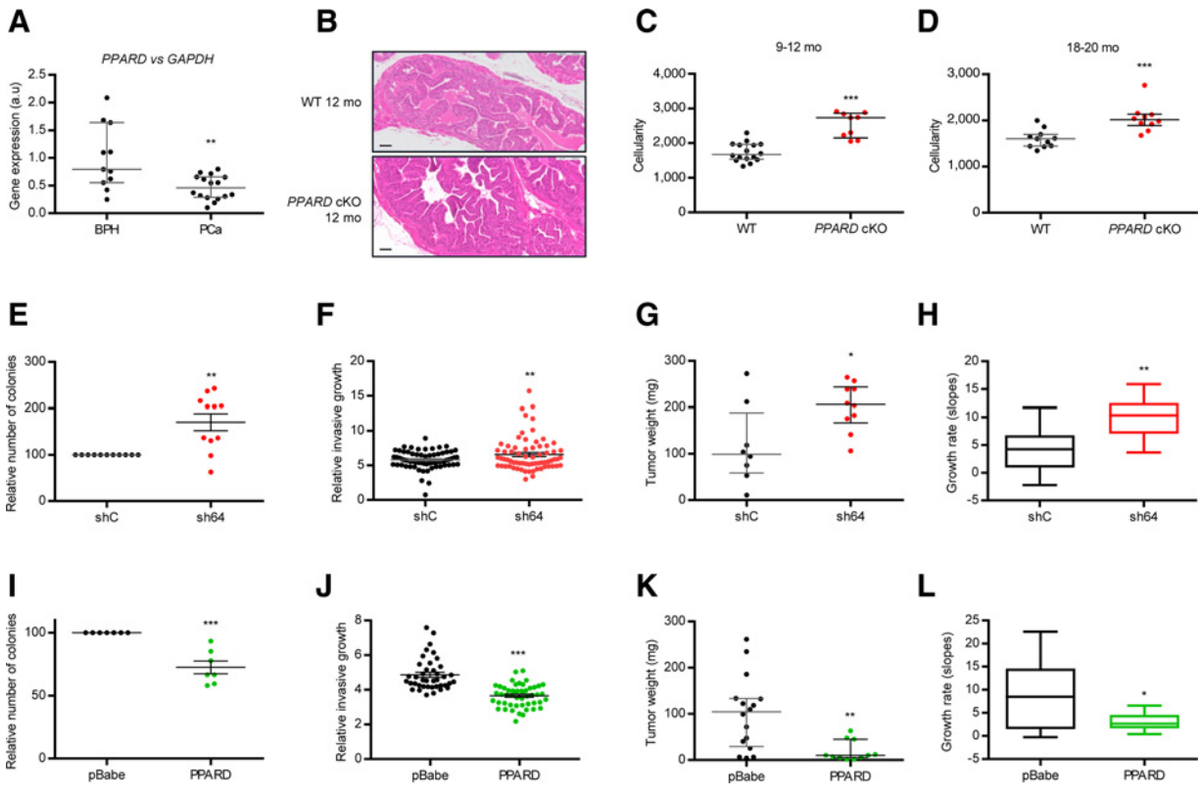

Figure 1.

PPARδ exhibits tumor suppressor activity. **A,** *PPARD* expression in prostate cancer (PCa; $n = 16$) and benign prostate hyperplasia (BPH; $n = 11$) patients. **B,** Representative images of H&E-stained tissues of wild-type (WT) and *PPARD* knock out (*PPARD* cKO) of 12-month-old mice. **C** and **D,** Quantitative assessment of the prostate glandular structures by counting the number of epithelial cells. Mean number of cells per mm^2 is represented as 9- to 12- and 18- to 20-month-old mice (9 months, $n = 16$; 12 months, $n = 9$; 18 months, $n = 11$; 20 months, $n = 10$). **E** and **F,** Effect of *PPARD* silencing with a short hairpin (sh64) in DU145 cells on anchorage independent growth ($n = 11$; **E**) and on the invasive growth capacity after 16 hours ($n = 3$; in each individual experiment, a mean of 20 colonies was counted and is represented in **F**). **G** and **H,** Impact of *PPARD* silencing in DU145 cells on tumor weight (**G**) and tumor growth rate ($n = 5$ mice; two injections per mouse; **H**). **I** and **J,** Effect of *PPARD* ectopic expression in PC3 cells on anchorage-independent growth ($n = 7$; **I**) and on the invasive growth capacity after 16 hours ($n = 3$; in each individual experiment, a mean of 20 colonies was counted and is represented in **J**. **K** and **L,** Impact of *PPARD* ectopic expression in PC3 cells on tumor weight (**K**) and tumor growth rate ($n = 5$ mice; four injections per mouse; **L**). Scale bar, 50 μm. Error bars, SEM. *, $P < 0.05$; **, $P < 0.01$; ***, $P < 0.001$ compared with control. Statistics test: two-tailed Student *t* test (**A**), one-tailed Mann–Whitney *U* test (**C**, **D**, **F–H**, **J–L**), one-sample *t* test (**E** and **I**). a.u., arbitrary units; shC, scramble shRNA.

vivo. Using subcutaneous xenografts, we observed that *PPARD* silencing in DU145 cells led to elevated tumor growth rate and tumor mass (Fig. 1G and H). Conversely, we overexpressed this gene with constitutive (pBabe-PPARD; Supplementary Fig. S1I–S1K) or inducible (TRIPZ-HA-PPARD) viral vectors (Supplementary Fig. S1L) and we evaluated the biological consequences. *PPARD* ectopic expression in PC3 cells resulted in reduced soft-agar colony formation and invasive growth (Fig. 1I and J; Supplementary Fig. S1M). Moreover, inoculation of PPARδ-expressing PC3 cells in the flank of immunocompromised mice resulted in reduced tumor growth rate and mass (Fig. 1K and L). It is worth noting a recent report that presented evidence of positive regulation of caveolin-1 (CAV1) downstream PPARδ leading to prostate cancer growth (22). However, we could not corroborate the biological nor the molecular results reported (Fig. 1; Supplementary Fig. S1N–S1P). Taken together, our results reveal that PPARδ expression decreased the aggressiveness of prostate cancer cells *in vitro* and *in vivo*, in line with the decrease in *PPARD* expression observed in human prostate cancer specimens.

The prostate tumor suppressive activity of PPARδ is ligand independent

PPARs exist in ligand-free and ligand-bound states. Unliganded PPARs have been reported to operate as a transcriptional repressor through the interaction with histone deacetylase complexes (HDAC), whereas ligand binding favors the release of HDACs and the interaction with histone acetyltransferases (HAT), leading to transcriptional activation (9, 23). One of the biochemical routes regulated by the transcriptional program downstream PPARD is FAO (24, 25). We evaluated the expression of canonical PPARδ target genes (*ADFP*, *ANGPTL4*, *PDK4*; ref. 26) and FAO. Interestingly, endogenous *PPARD* silencing increased both readouts (Fig. 2A and B, Supplementary Fig. S2A). Conversely, PPARδ overexpression in PC3 and LNCaP cells reduced the expression of these targets (Fig. 2C; Supplementary Fig. S2B–S2F) and inhibited FAO (Fig. 2D). We sought to validate these results in human specimens. Taking advantage of the previously presented sample set (Fig. 1A), we evaluated the mRNA levels of the aforementioned PPARδ targets and observed a significant upregulation (Fig. 2E–G). Furthermore, the negative correlation of PPARδ with these targets and the strong correlation among themselves supported the repressive activity reported *in vitro* (Fig. 2H–J; Supplementary Table S3). These results indicate that PPARD functions as a transcriptional repressor in prostate cancer probably owing to the lack of endogenous ligands in sufficient concentration, in agreement with other reports (27).

To ascertain whether ligand-bound PPARδ would switch to a transcriptional activator mode in prostate cancer, we treated control or *PPARD*-expressing PC3 cells with the synthetic agonist GW501516 (GW; ref. 24). GW treatment did not alter *PPARD* levels (Supplementary Fig. S2G) but switched the activity on its canonical targets from transcriptional repression to activation (Fig. 2K), which was accompanied by elevation of FAO (Fig. 2L). These results were validated with structurally unrelated synthetic PPARD ligands (Supplementary Fig. S2H–S2J). Of note, the direct regulation of these target genes by PPARδ was confirmed by ChIP analysis (Supplementary Fig. S2K–S2M).

Our results show that canonical PPARδ target regulation switches from transcriptional repression to activation based on ligand availability. Because we have shown that PPARD opposes prostate cancer growth, we asked whether PPARD agonists would also revert this tumor suppressive activity. Strikingly, PPARD-expressing PC3 cells treated with GW did not recover their ability to grow in anchorage-independent conditions (Fig. 2M). Overall, our results strongly suggest that the tumor suppressive activity of PPARδ in prostate cancer relies on an unprecedented ligand-independent function of the nuclear receptor.

The prostate tumor suppressive activity of PPARδ is DNA binding dependent

Because PPARδ regulates the vast majority of its biological activities through binding to DNA, we next studied to which extent the DNA binding capacity of this nuclear receptor was required for its biological activity. We generated a DNA binding mutant (DNA^{mut}) PPARδ (16), which we transduced into PC3 cells. As predicted, PPARδ-DNA^{mut} failed to mimic the activity of its WT counterpart on the regulation of canonical targets and FAO (Supplementary Fig. S3A–S3E). With regard to the biological activity, PPARδ-DNA^{mut} did not reduce soft-agar colony formation nor invasive growth (Fig. 3A and B). *In vivo*, PPARδ-DNA^{mut} expressing PC3 cells did not exhibit reduced tumor growth rate and mass compared with empty-vector transduced cells, and showed a significant recovery in these parameters compared with WT PPARδ-expressing counterparts (Fig. 3C and D). These data show that the tumor suppressive activity of PPARδ, which we report to be ligand independent, requires binding of the nuclear receptor to DNA.

PPARδ represses trefoil factor family gene expression to inhibit prostate cancer aggressiveness

Our results reveal that PPARδ exerts a tumor suppressive activity that is ligand-independent and DNA-binding dependent. Thus, we developed an experimental design to identify the transcriptional targets of this nuclear factor that would be potentially associated with this biological activity (Fig. 4A), based on two premises: (i) that their expression is regulated in PPARD overexpressing cells; (ii) that the type of regulation elicited by PPARD is not reverted in the presence of an agonist (thus ligand independent). On the one hand, we performed transcriptomics analysis with empty-vector transduced PC3 cells and *PPARD*-expressing counterparts. From this comparison, we focused on PPARδ-regulated genes. On the other hand, this approach was carried out with *PPARD*-expressing cells in the absence or presence of GW, which would allow us to rule out those genes regulated upon ligand binding. We therefore selected genes that presented a significant difference in expression upon PPARD expression (PC3-PPARD vs. PC3-pBabe, $P < 0.05$; $-1.5 >$ fold change > 1.5) that was retained also upon ligand treatment (PC3-PPARD + GW vs. PC3-pBabe, $P < 0.05$; $-1.5 >$ fold change > 1.5) as illustrated in Fig. 4A. This analysis led to the identification of candidate genes to mediate the ligand-independent activity of PPARδ. Surprisingly, the TFF stood among the top 10 genes downregulated by PPARD, which expression was not reverted by ligand treatment (Fig. 4B and Supplementary Table S4). We validated the repression of *TFF1* and *3* upon *PPARD* expression by real-time quantitative PCR, whereas *TFF2* expression was at the limit of detection (Fig. 4C; Supplementary Fig. S4A). As predicted from the experimental design, the repression of *TFF1* and *3* elicited by PPARδ expression was not reverted by the treatment with structurally unrelated ligands of the nuclear receptor (Fig. 4C;

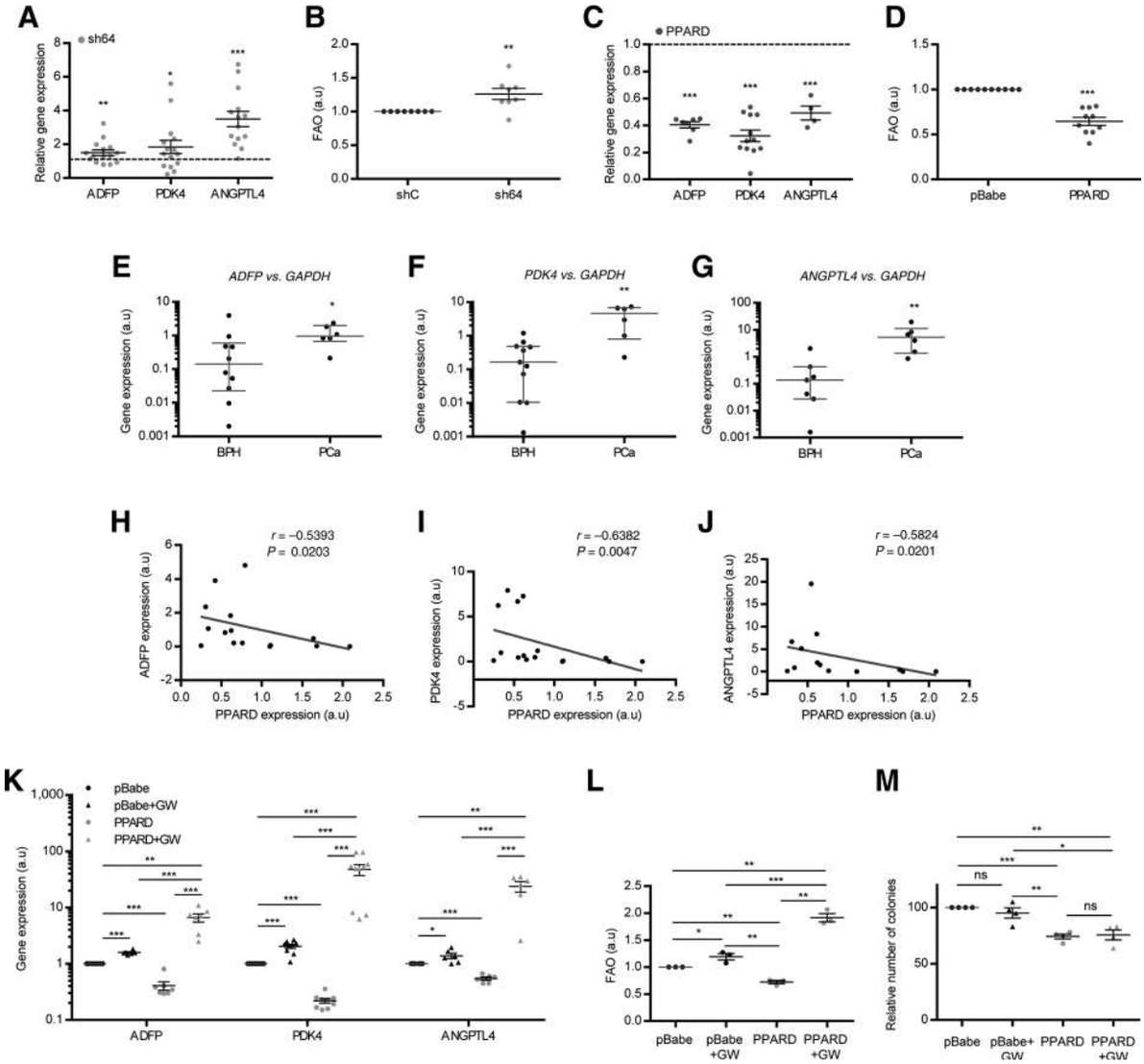

Figure 2.

PPARδ tumor suppressive activity is ligand independent. **A,** Expression of *PPARD* canonical target genes ($n = 15$) upon *PPARD* silencing with a short hairpin (sh64) in DU145 cells. **B,** Effect of *PPARD* silencing on FAO ($n = 8$) in DU145 cells. **C,** Expression of *PPARD* canonical target genes ($n = 15$) upon *PPARD* ectopic expression in PC3 cells. **D,** Effect of *PPARD* ectopic expression cells on FAO ($n = 10$) in PC3 cells. **E–G,** *PPARD* target gene expression, *ADFP* (**E**), *PDK4* (**F**), and *ANGPTL4* (**G**) in prostate cancer (PCa; $n = 16$) and benign prostate hyperplasia (BPH; $n = 11$) patients. **H–J,** Correlation analysis of *PPARD* expression with *ADFP* ($n = 15$; **H**), *PDK4* ($n = 16$; **I**), and *ANGPTL4* ($n = 13$; **J**) in prostate tissue used in **E–G** and Fig. 1A. **K–M,** Effect of PPARD synthetic ligand GW506015 (GW, 0.1 μmol/L, 48 hours) on *PPARD* canonical target genes expression (*ADFP,* $n = 7$; *PDK4,* $n = 10$; *ANGPTL4,* $n = 6$; **K**), on FAO ($n = 3$; **L**), and on anchorage-independent growth ($n = 4$; **M**) upon *PPARD* ectopic expression in PC3 cells. Error bars, SEM. *, $P < 0.05$; **, $P < 0.01$; ***, $P < 0.001$ compared with control. Statistics test: one sample *t* test when compared with control (**A–D** and **K–M**) and Student *t* test in two-component comparisons (**K–M**), one-tailed Mann–Whitney *U* test (**E–G**), and Spearman correlation (**H–J**). shC, scramble shRNA; a.u., arbitrary units.

Supplementary Fig. S4A–S4C). Conversely, *PPARD* silencing in DU145 cells resulted in increased *TFF1* expression (Fig. 4D). Importantly, *TFF1* and *3* were significantly upregulated in our cohort of prostate cancer specimens compared with benign prostate hyperplasia (Fig. 4E; Supplementary Fig. S4D). Deeper analysis of *PPARD* and *TFF* expression in patient-derived specimens revealed a significant inverse correlation between the expression of the nuclear factor and *TFF1*, but not *TFF3* (Fig. 4F; Supplementary Fig. S4E).

Our data show that PPARδ regulates the expression of *TFFs* in a ligand-independent manner. To elucidate whether this effect was direct on the promoter of the candidate genes, we performed ChIP with HA-tagged PPARD (Supplementary Fig. S4F and S4G). The analysis showed that this nuclear factor binds to the proximal region of *TFF1* and also to a large region of the *TFF3* promoter (Fig. 4G; Supplementary Fig. S4H). It is worth noting that the distal R6 region of TFF1 promoter did not exhibit any significant PPARD binding, thus acting as an internal negative control of the assay.

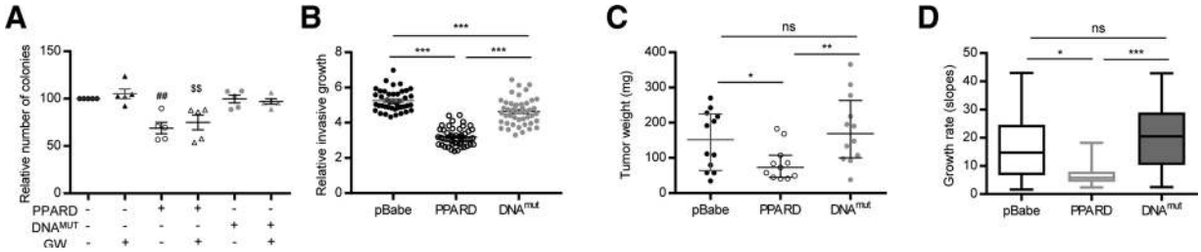

Figure 3.

PPARδ acts as a *cis* transcriptional repressor. **A,** Effect of PPARD synthetic ligand GW506015 (GW, 0.1 μmol/L, 48 hours) on anchorage independent growth ($n = 5$) upon *PPARD* and *PPARD* DNA^{mut} (DNA^{mut}) ectopic expression in PC3 cells. **B–D,** Effect of *PPARD* DNA^{mut} on the invasive growth capacity ($n = 3$, in which in each individual experiment, a mean of 20 colonies was counted and is represented in **B**), on tumor weight (**C**), and tumor growth rate ($n = 3$ mice; four injections per mouse; **D**) upon *PPARD* and *PPARD* DNA^{mut} (DNA^{mut}) ectopic expression in PC3 cells. Error bars, SEM. *, $P < 0.05$; **, $P < 0.01$; ***, $P < 0.001$ as indicated; #, compared with pBABE; $, compared with. pBABE + GW. Statistics test: one sample *t* test when compared with control (**A**) and Student *t* test in two-component comparisons (**A**) and one-tailed Mann–Whitney *U* test (**B–D**). ns, not significant.

TFFs are secreted proteins that act on cellular signaling through poorly defined mechanisms (28). In order to elucidate the contribution of *TFF1* to prostate cancer, we overexpressed TFF1 in DU145 cells using an inducible (TRIPZ-TFF1) viral vector (Supplementary Fig. S5A and S5B) and observed increased soft-agar colony formation *in vitro* (Fig. 5A) and tumor growth rate and mass *in vivo* (Fig. 5B and C).

Next, we ascertained the requirements of TFF1 regulation for the tumor suppressive activity of PPARδ. On the one hand, we treated *PPARD*-expressing cells with recombinant human TFF1

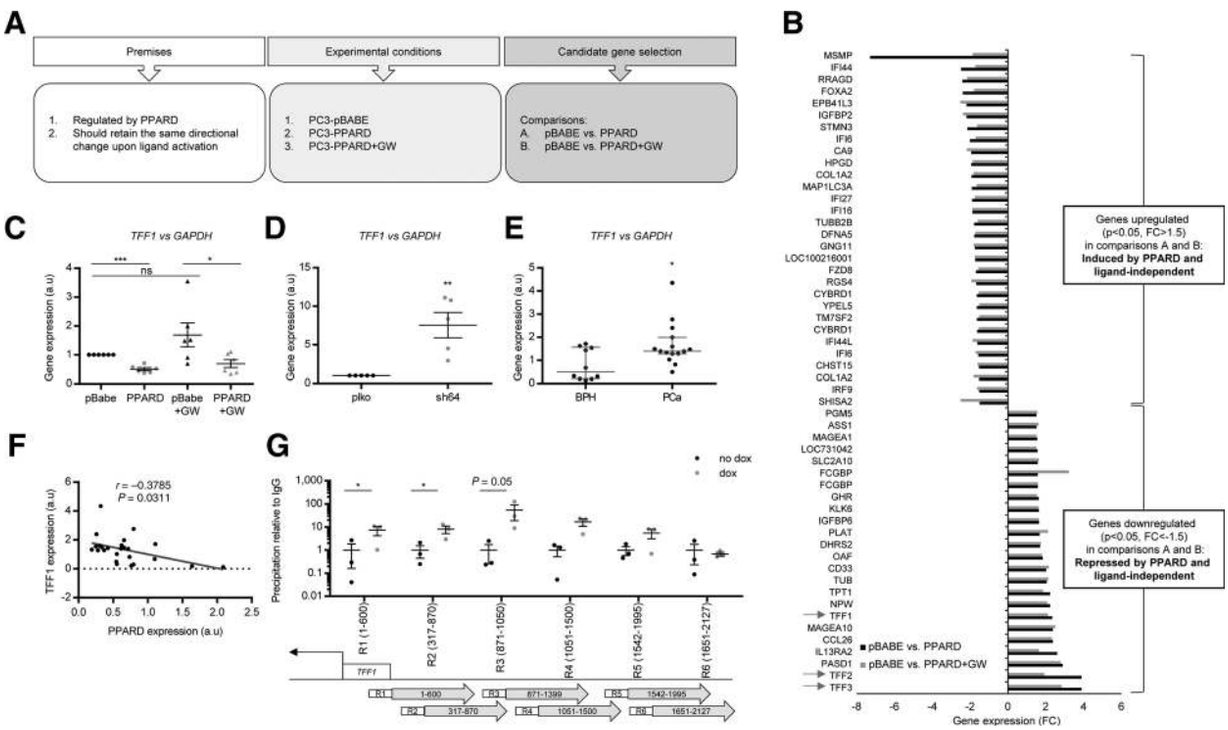

Figure 4.

PPARδ represses TFF1 independently of ligand. **A,** Data processing diagram from the microarray analysis carried out in pBabe, *PPARD*, and *PPARD* + GW (0.1 μmol/L, 48 hours) PC3 cells ($n = 3$ per group). **B,** Fold change (FC) expression of PPARδ upregulated and downregulated genes independently of ligand obtained in **A**. Arrows, members of the *TFF*. **C,** Effect of PPARD synthetic ligand GW506015 (GW, 0.1 μmol/L, 48 hours) on *TFF1* gene expression ($n = 6$) in PC3 cells upon PPARD ectopic expression. **D,** *TFF1* gene expression ($n = 5$) upon *PPARD* silencing with a short hairpin (sh64) in DU145 cells. **E,** *TFF1* gene expression in prostate cancer (PCa; $n = 15$) and benign prostate hyperplasia (BPH; $n = 10$) patients. **F,** Correlation analysis of *TFF1* and *PPARD* gene expression in cancer and benign prostate hyperplasia patients ($n = 25$). **G,** ChIP of exogenous HA-PPARD on *TFF1* promoter using HA-tag antibody in PC3 cells after induction with 0.5 μg/mL doxycycline for 3 days ($n = 3$). Data were normalized to IgG (negative-binding control). Bottom, the different regions (R1-R6) chosen for the analysis of PPARD occupancy. R6, negative binding control. Error bars, SEM. *, $P < 0.05$; ***, $P < 0.001$ compared with control. Statistics test: one sample *t* test when compared with control (**C** and **D**) and Student *t* test in two-component comparisons (**C**), one-tailed Mann–Whitney *U* test (**E**), Spearman correlation (**F**), and one-tailed Student *t* test (**G**). ns, not significant; a.u., arbitrary units; dox, doxycycline.

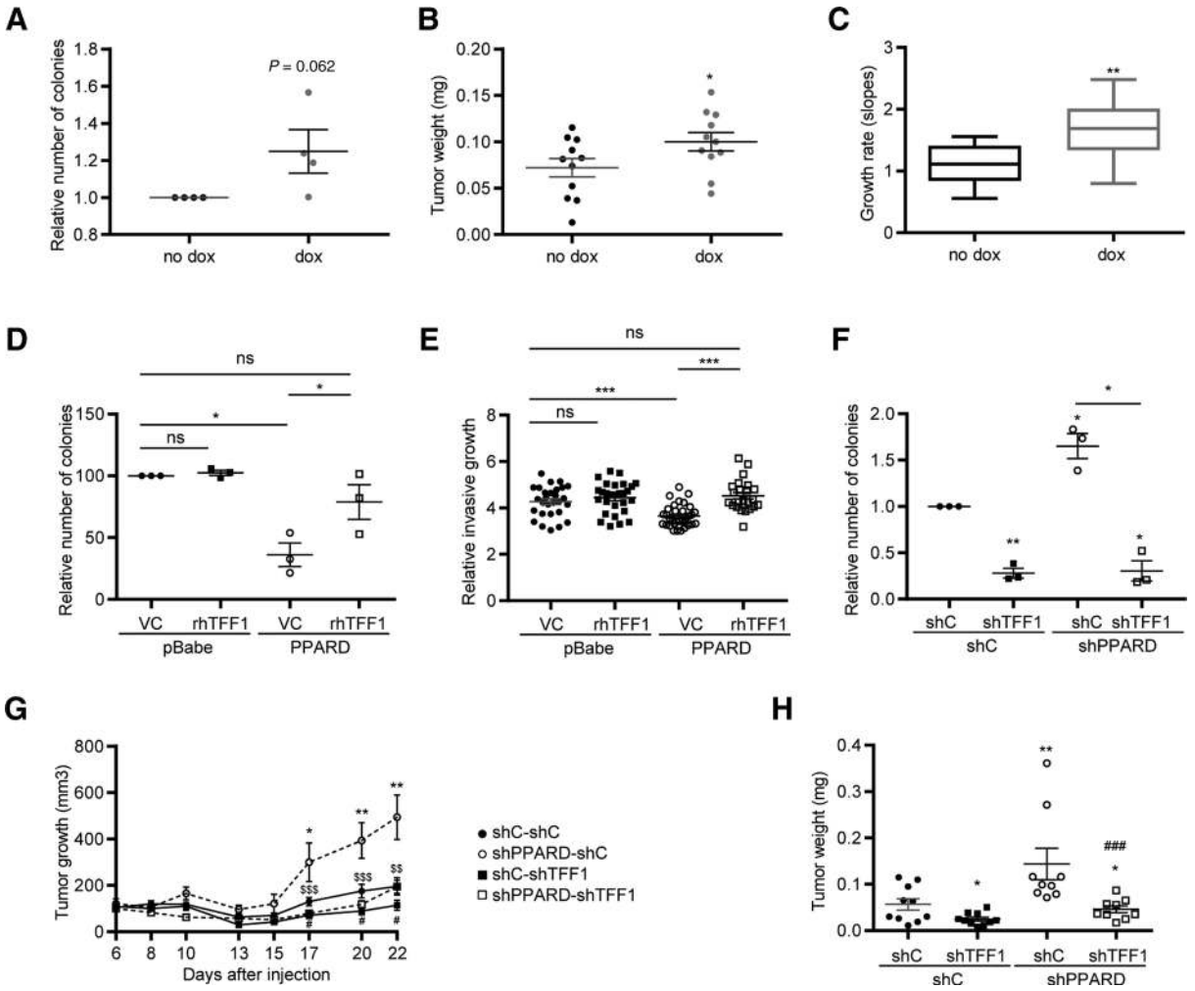

Figure 5.

TFF1 downregulation contributes to the tumor suppressive activity of PPARδ in prostate cancer. **A,** Effect of *TFF1* ectopic expression (induction with 0.5 μg/mL doxycyclin) in DU145 cells on anchorage-independent growth ($n = 4$). **B** and **C,** Effect of *TFF1* conditional overexpression in established prostate tumors of DU145 cells on tumor weight (**B**) and tumor growth rate ($n = 6$ mice; two injections per mouse; **C**). Doxycycline diet was given to the treatment group on day 12 after xenograft injection when tumors reached 100 mm^3. **D** and **E,** Effect of recombinant human TFF1 protein (rhTFF1) on anchorage-independent growth ($n = 3$; **D**) and on the invasive growth capacity ($n = 3$; in each individual experiment, a mean of 10 colonies was counted and is represented in **E**) upon *PPARD* ectopic expression in PC3 cells. **F–H,** Effect of *TFF1* silencing with a short hairpin (shTFF1) upon *PPARD* silencing with a short hairpin (shPPARD, previously identified as sh64) in DU145 cells *in vitro* on anchorage-independent growth ($n = 3$; **F**) and *in vivo* in tumor growth and mass ($n = 5$ mice; two flanks per mouse; **G** and **H**). shC, pLKO lentiviral vector expressing scramble shRNA; VC, vehicle control. Error bars, SEM; $^{*/\#/\$}$, $P < 0.05$; $^{**/\#\#/\$\$}$, $P < 0.01$; $^{***/\#\#\#/\$\$\$}$, $P < 0.001$. For **G**: *, shPPARD-shC vs. shC-shC; #, shTFF1-shC vs. shC-shC; $, shPPARD-shC vs. shC-shC; for **H**: *, indicated condition vs. shC-shC; #, indicated condition vs. shPPARD-shC. Statistics test: one-sample *t* test when compared with control (**A**, **D**, **F**) and Student *t* test in two-component comparisons (**D** and **F**), one-tailed Mann–Whitney *U* test (**B**, **C**, **E**, **G**, **H**); ns, not significant; a.u., arbitrary units; dox, doxycycline.

(rhTFF1) protein. As predicted, rhTFF1 partially rescued the defect of *PPARD*-expressing cells in anchorage-independent growth (Fig. 5D) and invasive growth (Fig. 5E). On the other hand, we transduced DU145 cells carrying constitutive scramble or *PPARD* shRNAs with *TFF1* shRNA-expressing lentivirus (or scramble shRNA expressing controls; the efficacy of *TFF1* silencing was tested in the TFF1 high-expressing PC3 cell line; Supplementary Fig. S5C and S5D). The results confirmed that *TFF1*-silenced cells exhibited reduced colony forming ability and tumor growth, and, importantly, failed to show the elevation in this parameter elicited by *PPARD* shRNA (Fig. 5F–H). Overall, our data provide evidence of a tumor suppressive activity of PPARδ stemming from the ligand-independent regulation of TFF1 in prostate cancer.

Discussion

The physiological activity of PPARδ has been described in great detail (9–11). However, its role in cancer remains controversial. In addition, conclusions of PPARδ activity based on the use of synthetic agonists have added complexity to its biological activity. It has been reported that activation of PPARδ by synthetic ligands such as GW501516 or GW0742 promotes oncogenesis in prostate, thyroid, breast cancer, or liposarcoma cells, whereas

antagonizing PPARδ inhibits tumorigenesis in lung, liver, breast, or prostate cell lines (29–31). Conversely, various studies have demonstrated that the activation of PPARδ by agonists reverts or inhibits tumorigenesis in colorectal, liver, skin, breast, testicular, pancreatic cancer, or neuroblastoma cells (32–39), in line with the notion that the deregulation of this nuclear receptor promotes oncogenesis in *Ppard*-deficient mice and colorectal cancer cells (40, 41). The expression status of PPARδ in cancer has been evaluated by different groups with contrasting results, which may be related to the tissue of origin and the method for quantification of *PPARD* levels (42–44). Importantly, the publication of the Human Protein Atlas portal (44) allowed a comprehensive analysis of PPARδ protein expression in different tissues and demonstrated a lower expression of this nuclear receptor in prostate, colorectal, urethral, liver, breast or ovarian cancer, among others. Our results provide evidence for a decrease of PPARδ expression in prostate cancer that has consequences on the biology of the disease, suggesting that tumor suppression could be a major role for this nuclear receptor in the prostate epithelium.

The vast majority of effects elicited by PPARδ depend on specific ligands binding to the ligand binding domain (LBD) of the nuclear factor (9). However, recent studies report transcriptional activity of PPARδ that does not require ligand challenge. First, PPARδ-regulated transcriptional repression of ANGPTL4 mediates tumor suppression in breast cancer (27). Interestingly, the authors identify in this study 105 genes that are sensitive to *PPARD* silencing but not to the effect of agonists or inverse agonists. Second, an extensive study on the transcriptional regulation by PPARδ in keratinocytes identified different modes of action of this nuclear receptor (13). Importantly, a significant number of genes in this study presented a regulation by PPARδ that was constitutive and ligand independent, suggesting that this factor could crosstalk with other transcriptional regulators (13). Our results provide evidence for a repressive and ligand-independent activity of PPARδ in prostate cancer that drives tumor suppression.

The TFF comprises three members that were identified as secreted factors produced by cells in mucosa. Interestingly, the function of TFFs has been related to inflammation, proliferation, and invasiveness, and these factors have been categorized as growth factor-like molecules. The alteration of TFF expression has been widely studied and reviewed (28, 45), and there is an overall consensus that these proteins are overexpressed in tumors, with a few exceptions. In prostate cancer TFF1 and 3 are upregulated and have been proposed as tissue and body fluid cancer biomarkers (46–52). Moreover, experimental evidence demonstrate that expression of TFF1 and 3 in prostate cancer increases oncogenicity by means of proliferation, survival, anchorage-independent growth, and invasiveness (53, 54), which we validate in our experimental systems *in vitro* and *in vivo*. Yet, little is known about their regulation. The upregulation has been addressed at different levels, and hypomethylation of the promoter has been postulated as a mechanism in prostate cancer (45, 55). Our results show that PPARδ is a negative regulator of TFF expression, which could contribute the upregulation of TFFs observed in prostate cancer.

TFF regulation by PPARδ in a ligand-independent manner would allow the uncoupling of its ligand-dependent physiological activities from tumor-suppressive constitutive functions of the nuclear factor. This new perspective opens new and exciting opportunities to elucidate the dualities of this family of nuclear receptors in cancer.

Disclosure of Potential Conflicts of Interest

No potential conflicts of interest were disclosed.

Authors' Contributions

Conception and design: N. Martín-Martín, A. Carracedo
Development of methodology: N. Martín-Martín, A. Zabala-Letona, V. Torrano, M. Unda, A.M. Aransay, R. Barrio, J.D. Sutherland, A. Carracedo
Acquisition of data (provided animals, acquired and managed patients, provided facilities, etc.): M. Castillo-Martin, A. Loizaga-Iriarte, M. Unda, A.M. Aransay
Analysis and interpretation of data (e.g., statistical analysis, biostatistics, computational analysis): N. Martín-Martín, A.R. Cortazar, V. Torrano, A.M. Aransay, A. Carracedo
Writing, review, and/or revision of the manuscript: N. Martín-Martín, A. Carracedo
Administrative, technical, or material support (i.e., reporting or organizing data, constructing databases): A.R. Cortazar, P. Sanchez-Mosquera, A.M. Aransay
Study supervision: A. Carracedo
Other (contributed to *in vitro* and/or *in vivo* analysis): A. Zabala-Letona, L. Arreal, L. Camacho, P. Zuñiga-Garcia, L. Valcarcel-Jimenez, A. Arruabarrena-Aristorena, M. Piva
Other (performed the histochemical staining and *in vitro* analyses): S. Fernandez-Ruiz
Other (mouse uropathology): M. Castillo
Other (human uropathology): A. Ugalde-Olano
Other (development of TFF1-related molecular tools): I. Astobiza
Other (co-supervision of L. Camacho): A. Gomez-Muñoz

Acknowledgments

Apologies to those whose related publications were not cited due to space limitations. N. Martin-Martin is supported by the Spanish Association Against Cancer (AECC), AECC JP Vizcaya. L. Arreal, A. Arruabarrena-Aristorena, and L. Valcarcel-Jimenez are supported by the Basque Government of Education. R. Barrio acknowledges Spanish MINECO (BFU2014-52282-P, Consolider BFU2014-57703-REDC), the Departments of Education and Industry of the Basque Government (PI2012/42) and the Bizkaia County. The work of A. Carracedo is supported by the Basque Department of Industry, Tourism and Trade (Etortek) and the Department of Education (IKERTALDE IT1106-16, also participated by A. Gomez-Muñoz), the BBVA Foundation, the MINECO (SAF2016-79381-R (FEDER/EU); Severo Ochoa Excellence Accreditation (SEV-2016-0644) and the European Research Council (Starting Grant 336343, PoC 754627). CIBERONC was co-funded with FEDER funds. We are thankful to the Basque Biobank for Research (BIOEF) for the support in the acquisition and management of human specimens.

The costs of publication of this article were defrayed in part by the payment of page charges. This article must therefore be hereby marked *advertisement* in accordance with 18 U.S.C. Section 1734 solely to indicate this fact.

Received March 30, 2017; revised September 18, 2017; accepted November 14, 2017; published OnlineFirst November 29, 2017.

References

1. Vander Heiden MG, Cantley LC, Thompson CB. Understanding the Warburg effect: the metabolic requirements of cell proliferation. Science 2009;324:1029–33.
2. Torrano V, Valcarcel-Jimenez L, Cortazar AR, Liu X, Urosevic J, Castillo-Martin M, et al. The metabolic co-regulator PGC1alpha suppresses prostate cancer metastasis. Nat Cell Biol 2016;18:645–56.

3. Kypta R, Unda M, Carracedo A. Is the bench getting closer to the bedside in the war on cancer? A quick look at prostate cancer. Front Endocrinol 2012;3:53.
4. Braissant O, Foufelle F, Scotto C, Dauca M, Wahli W. Differential expression of peroxisome proliferator-activated receptors (PPARs): tissue distribution of PPAR-alpha, -beta, and -gamma in the adult rat. Endocrinology 1996;137:354–66.
5. Takahashi S, Tanaka T, Sakai J. New therapeutic target for metabolic syndrome: PPARdelta. Endocr J 2007;54:347–57.
6. Feige JN, Gelman L, Michalik L, Desvergne B, Wahli W. From molecular action to physiological outputs: peroxisome proliferator-activated receptors are nuclear receptors at the crossroads of key cellular functions. Prog Lipid Res 2006;45:120–59.
7. Varga T, Czimmerer Z, Nagy L. PPARs are a unique set of fatty acid regulated transcription factors controlling both lipid metabolism and inflammation. Biochim Biophys Acta 2011;1812:1007–22.
8. Glass CK, Ogawa S. Combinatorial roles of nuclear receptors in inflammation and immunity. Nat Rev Immunol 2006;6:44–55.
9. Peters JM, Shah YM, Gonzalez FJ. The role of peroxisome proliferator-activated receptors in carcinogenesis and chemoprevention. Nat Rev Cancer 2012;12:181–95.
10. Peters JM, Gonzalez FJ, Muller R. Establishing the role of PPARbeta/delta in carcinogenesis. Trends Endocrinol Metab 2015;26:595–607.
11. Peters JM, Yao PL, Gonzalez FJ. Targeting peroxisome proliferator-activated receptor-beta/delta (PPARbeta/delta) for cancer chemoprevention. Curr Pharmacol Rep 2015;1:121–8.
12. Adhikary T, Kaddatz K, Finkernagel F, Schonbauer A, Meissner W, Scharfe M, et al. Genomewide analyses define different modes of transcriptional regulation by peroxisome proliferator-activated receptor-beta/delta (PPARbeta/delta). PLoS One 2011;6:e16344.
13. Khozoie C, Borland MG, Zhu B, Baek S, John S, Hager GL, et al. Analysis of the peroxisome proliferator-activated receptor-beta/delta (PPARbeta/delta) cistrome reveals novel co-regulatory role of ATF4. BMC Genomics 2012;13:665.
14. Morgenstern JP, Land H. Advanced mammalian gene transfer: high titre retroviral vectors with multiple drug selection markers and a complementary helper-free packaging cell line. Nucleic Acids Res 1990;18:3587–96.
15. Brun RP, Tontonoz P, Forman BM, Ellis R, Chen J, Evans RM, et al. Differential activation of adipogenesis by multiple PPAR isoforms. Genes Dev 1996;10:974–84.
16. Shi Y, Hon M, Evans RM. The peroxisome proliferator-activated receptor delta, an integrator of transcriptional repression and nuclear receptor signaling. Proc Natl Acad Sci U S A 2002;99:2613–8.
17. Carracedo A, Weiss D, Leliaert AK, Bhasin M, de Boer VC, Laurent G, et al. A metabolic prosurvival role for PML in breast cancer. J Clin Invest 2012;122:3088–100.
18. Barak Y, Liao D, He W, Ong ES, Nelson MC, Olefsky JM, et al. Effects of peroxisome proliferator-activated receptor delta on placentation, adiposity, and colorectal cancer. Proc Natl Acad Sci U S A 2002;99:303–8.
19. Chen Z, Trotman LC, Shaffer D, Lin HK, Dotan ZA, Niki M, et al. Crucial role of p53-dependent cellular senescence in suppression of Pten-deficient tumorigenesis. Nature 2005;436:725–30.
20. Ugalde-Olano A, Egia A, Fernandez-Ruiz S, Loizaga-Iriarte A, Zuniga-Garcia P, Garcia S, et al. Methodological aspects of the molecular and histological study of prostate cancer: focus on PTEN. Methods 2015; 77–78:25–30.
21. Rhodes DR, Yu J, Shanker K, Deshpande N, Varambally R, Ghosh D, et al. ONCOMINE: a cancer microarray database and integrated data-mining platform. Neoplasia 2004;6:1–6.
22. Her NG, Jeong SI, Cho K, Ha TK, Han J, Ko KP, et al. PPARdelta promotes oncogenic redirection of TGF-beta1 signaling through the activation of the ABCA1-Cav1 pathway. Cell Cycle 2013;12:1521–35.
23. Evans RM, Barish GD, Wang YX. PPARs and the complex journey to obesity. Nat Med 2004;10:355–61.
24. Ito K, Carracedo A, Weiss D, Arai F, Ala U, Avigan DE, et al. A PML–PPAR-δ pathway for fatty acid oxidation regulates hematopoietic stem cell maintenance. Nat Med 2012;18:1350–8.
25. Carracedo A, Cantley LC, Pandolfi PP. Cancer metabolism: fatty acid oxidation in the limelight. Nat Rev Cancer 2013;13:227–32.
26. Peters JM, Foreman JE, Gonzalez FJ. Dissecting the role of peroxisome proliferator-activated receptor-beta/delta (PPARbeta/delta) in colon, breast, and lung carcinogenesis. Cancer Metastasis Rev 2011;30:619–40.
27. Adhikary T, Brandt DT, Kaddatz K, Stockert J, Naruhn S, Meissner W, et al. Inverse PPARbeta/delta agonists suppress oncogenic signaling to the ANGPTL4 gene and inhibit cancer cell invasion. Oncogene 2013;32: 5241–52.
28. Kjellev S. The trefoil factor family - small peptides with multiple functionalities. Cell Mol Life Sci 2009;66:1350–69.
29. Stephen RL, Gustafsson MC, Jarvis M, Tatoud R, Marshall BR, Knight D, et al. Activation of peroxisome proliferator-activated receptor delta stimulates the proliferation of human breast and prostate cancer cell lines. Cancer Res 2004;64:3162–70.
30. Wagner KD, Benchetrit M, Bianchini L, Michiels JF, Wagner N. Peroxisome proliferator-activated receptor beta/delta (PPARbeta/delta) is highly expressed in liposarcoma and promotes migration and proliferation. J Pathol 2011;224:575–88.
31. Zeng L, Geng Y, Tretiakova M, Yu X, Sicinski P, Kroll TG. Peroxisome proliferator-activated receptor-delta induces cell proliferation by a cyclin E1-dependent mechanism and is up-regulated in thyroid tumors. Cancer Res 2008;68:6578–86.
32. Bility MT, Devlin-Durante MK, Blazanin N, Glick AB, Ward JM, Kang BH, et al. Ligand activation of peroxisome proliferator-activated receptor beta/delta (PPAR beta/delta) inhibits chemically induced skin tumorigenesis. Carcinogenesis 2008;29:2406–14.
33. Coleman JD, Thompson JT, Smith RW 3rd, Prokopczyk B, Vanden Heuvel JP. Role of peroxisome proliferator-activated receptor beta/delta and B-cell lymphoma-6 in regulation of genes involved in metastasis and migration in pancreatic cancer cells. PPAR Res 2013;2013:121956.
34. Foreman JE, Sharma AK, Amin S, Gonzalez FJ, Peters JM. Ligand activation of peroxisome proliferator-activated receptor-beta/delta (PPARbeta/delta) inhibits cell growth in a mouse mammary gland cancer cell line. Cancer Lett 2010;288:219–25.
35. Harman FS, Nicol CJ, Marin HE, Ward JM, Gonzalez FJ, Peters JM. Peroxisome proliferator-activated receptor-delta attenuates colon carcinogenesis. Nat Med 2004;10:481–3.
36. Hollingshead HE, Killins RL, Borland MG, Girroir EE, Billin AN, Willson TM, et al. Peroxisome proliferator-activated receptor-beta/delta (PPAR-beta/delta) ligands do not potentiate growth of human cancer cell lines. Carcinogenesis 2007;28:2641–9.
37. Yao PL, Chen L, Dobrzanski TP, Zhu B, Kang BH, Muller R, et al. Peroxisome proliferator-activated receptor-beta/delta inhibits human neuroblastoma cell tumorigenesis by inducing p53- and SOX2-mediated cell differentiation. Mol Carcinog 2017;56:1472–83.
38. Yao PL, Chen LP, Dobrzanski TP, Phillips DA, Zhu B, Kang BH, et al. Inhibition of testicular embryonal carcinoma cell tumorigenicity by peroxisome proliferator-activated receptor-beta/delta- and retinoic acid receptor-dependent mechanisms. Oncotarget 2015;6:36319–37.
39. Yao PL, Morales JL, Zhu B, Kang BH, Gonzalez FJ, Peters JM. Activation of peroxisome proliferator-activated receptor-beta/delta (PPAR-beta/delta) inhibits human breast cancer cell line tumorigenicity. Mol Cancer Ther 2014;13:1008–17.
40. Muller-Brusselbach S, Ebrahimsade S, Jakel J, Eckhardt J, Rapp UR, Peters JM, et al. Growth of transgenic RAF-induced lung adenomas is increased in mice with a disrupted PPARbeta/delta gene. Int J Oncol 2007;31:607–11.
41. Yang L, Olsson B, Pfeifer D, Jonsson JI, Zhou ZG, Jiang X, et al. Knockdown of peroxisome proliferator-activated receptor-beta induces less differentiation and enhances cell-fibronectin adhesion of colon cancer cells. Oncogene 2010;29:516–26.
42. He TC, Chan TA, Vogelstein B, Kinzler KW. PPARdelta is an APC-regulated target of nonsteroidal anti-inflammatory drugs. Cell 1999;99: 335–45.
43. Modica S, Gofflot F, Murzilli S, D'Orazio A, Salvatore L, Pellegrini F, et al. The intestinal nuclear receptor signature with epithelial localization patterns and expression modulation in tumors. Gastroenterology 2010; 138:636–48, 48 e1–12.
44. Uhlen M, Fagerberg L, Hallstrom BM, Lindskog C, Oksvold P, Mardinoglu A, et al. Proteomics. Tissue-based map of the human proteome. Science 2015;347:1260419.
45. Busch M, Dunker N. Trefoil factor family peptides–friends or foes? Biomol Concepts 2015;6:343–59.

46. Abdou AG, Aiad HA, Sultan SM. pS2 (TFF1) expression in prostate carcinoma: correlation with steroid receptor status. APMIS 2008;116:961–71.
47. Faith DA, Isaacs WB, Morgan JD, Fedor HL, Hicks JL, Mangold LA, et al. Trefoil factor 3 overexpression in prostatic carcinoma: prognostic importance using tissue microarrays. Prostate 2004;61:215–27.
48. Garraway IP, Seligson D, Said J, Horvath S, Reiter RE. Trefoil factor 3 is overexpressed in human prostate cancer. Prostate 2004;61: 209–14.
49. Liu M, Jin RS. [Expressions of TFF1 and TFF3 in prostate cancer and prostatic intraepithelial neoplasia and their clinical significance]. Zhonghua Nan Ke Xue 2015;21:315–9.
50. Park K, Chiu YL, Rubin MA, Demichelis F, Mosquera JM. V-ets erythroblastosis virus E26 oncogene homolog (avian)/Trefoil factor 3/high-molecular-weight cytokeratin triple immunostain: a novel tissue-based biomarker in prostate cancer with potential clinical application. Hum Pathol 2013;44:2282–92.
51. Terry S, Nicolaiew N, Basset V, Semprez F, Soyeux P, Maille P, et al. Clinical value of ERG, TFF3, and SPINK1 for molecular subtyping of prostate cancer. Cancer 2015;121:1422–30.
52. Vestergaard EM, Borre M, Poulsen SS, Nexo E, Torring N. Plasma levels of trefoil factors are increased in patients with advanced prostate cancer. Clin Cancer Res 2006;12:807–12.
53. Bougen NM, Amiry N, Yuan Y, Kong XJ, Pandey V, Vidal LJ, et al. Trefoil factor 1 suppression of E-CADHERIN enhances prostate carcinoma cell invasiveness and metastasis. Cancer Lett 2013;332:19–29.
54. Perera O, Evans A, Pertziger M, MacDonald C, Chen H, Liu DX, et al. Trefoil factor 3 (TFF3) enhances the oncogenic characteristics of prostate carcinoma cells and reduces sensitivity to ionising radiation. Cancer Lett 2015;361:104–11.
55. Vestergaard EM, Nexo E, Torring N, Borre M, Orntoft TF, Sorensen KD. Promoter hypomethylation and upregulation of trefoil factors in prostate cancer. Int J Cancer 2010;127:1857–65.